Computational discovery of p-type transparent oxide semiconductors using hydrogen descriptor

Kanghoon Yim[1,*,†], Yong Youn[1,*], Miso Lee[1,] Dongsun Yoo[1], Joohee Lee[1], Sung Haeng Cho[2] & Seungwu Han[1]

[1]Department of Materials Science and Engineering and Research Institute of Advanced Materials, Seoul National University, Seoul 08826, Korea

[2]Electronics and Telecommunications Research Institute (ETRI), Daejeon 34129, Korea

[†]Present address: Korea Institute of Energy Research, Daejeon 305-343, Korea

* These authors contributed equally to this work.

Contact information: Seungwu Han / hansw@snu.ac.kr

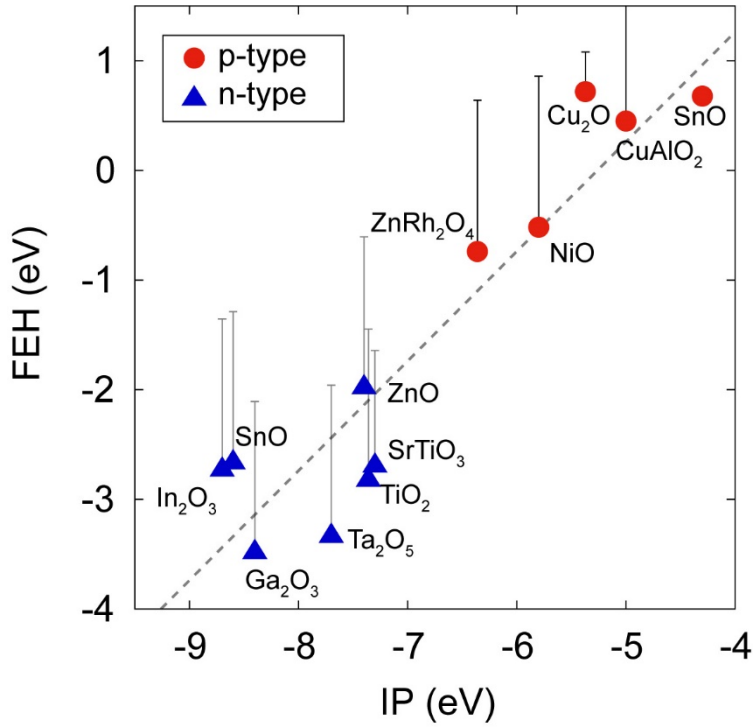

Figure S1. FEH versus experimental ionization potential. The grey error-bars represent the variation of FEH with O_2 pressure under the condition that each phase is stable. The upper (lower) limit of each error bar corresponds to the oxygen-rich (oxygen-poor) conditions.[1-4]

If the material is stable in all O_2 partial pressure (P_{O2}), the hydrogen chemical potential can differ by up to1.38 eV (highest in the O-rich condition). However, P_{O2} is often limited in the range where the considered material is stable. For example, SnO is not stable even in a very low oxygen chemical potential since SnO_2 phase is very stable. To avoid the complexity involved in determining the oxygen chemical potential, we defined FEH by fixing the hydrogen chemical potential to that of H_2 gas (i.e., O-poor condition). If we instead considered O-rich condition in calculating FEH, the values can vary as the shown in Fig. S1. Even if we use the highest FEH values in Fig. S1, it is seen that the p-type oxides still cluster in the region of FEH > 0 eV.

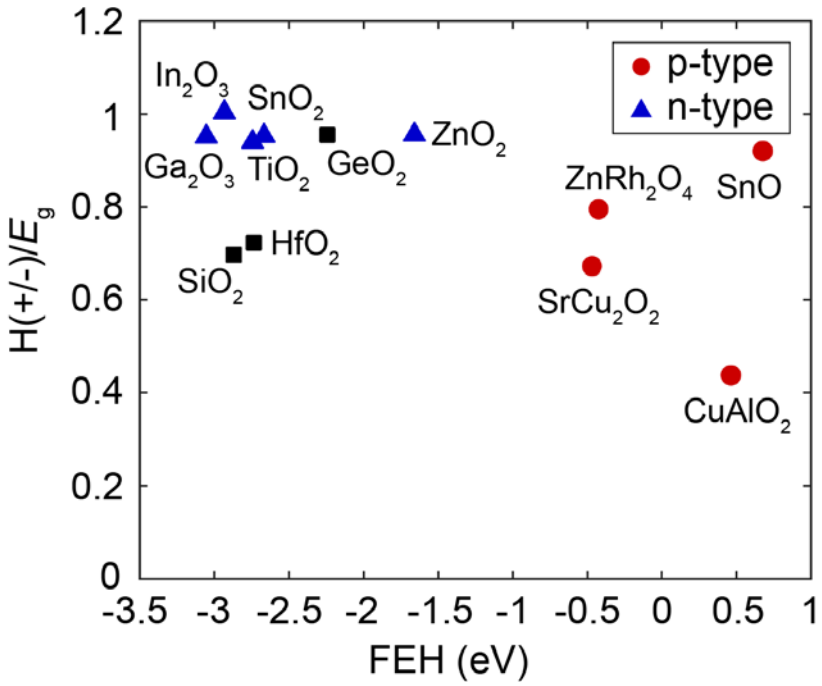

Figure S2. FEH versus H(+/−)/E_g level computed within the hybrid functional.

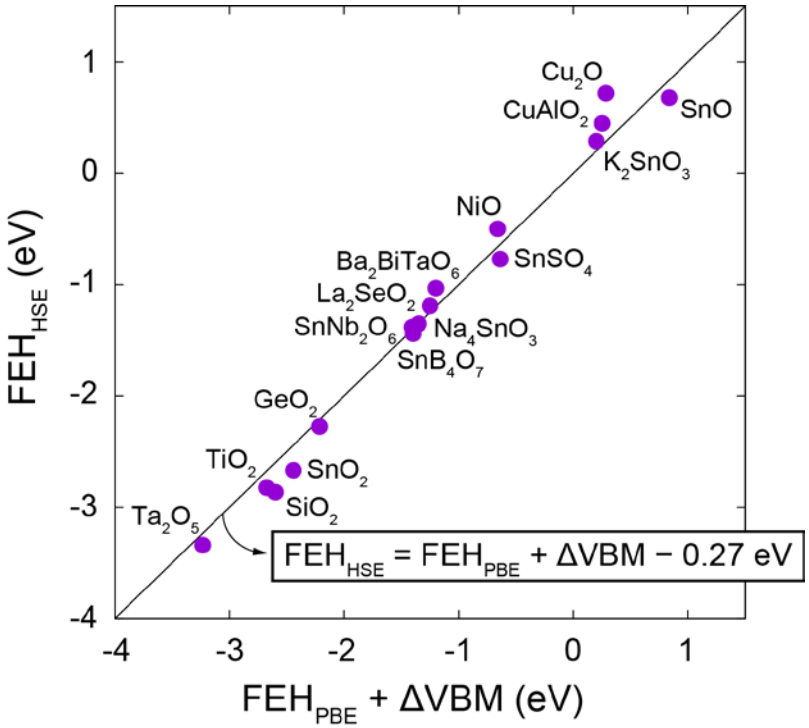

Figure S3. Comparison of FEH using PBE functional with VBM correction and full HSE functional.

Stable H_i^+ site in oxides. To search the stable H_i^+ site in oxides, we test various configurations including anti-bonding sites, bond-center sites, and void sites found from Voronoi vertices. As an example, supercell of $SnNb_2O_6$ and the relaxed H_i^+ sites starting from the various initial configurations are shown in Fig. S4. We find that the H_i^+ always prefer to form O-H bond through relaxation and the most stable O-H bond is lie in the direction of the maximum Coulomb potential around the oxygen in all our test calculations. We also test the cases of multiple anion system such as La_2O_2Te and LaCuOSe and confirm that O-H bond is always more stable than the bond with other anion atoms.

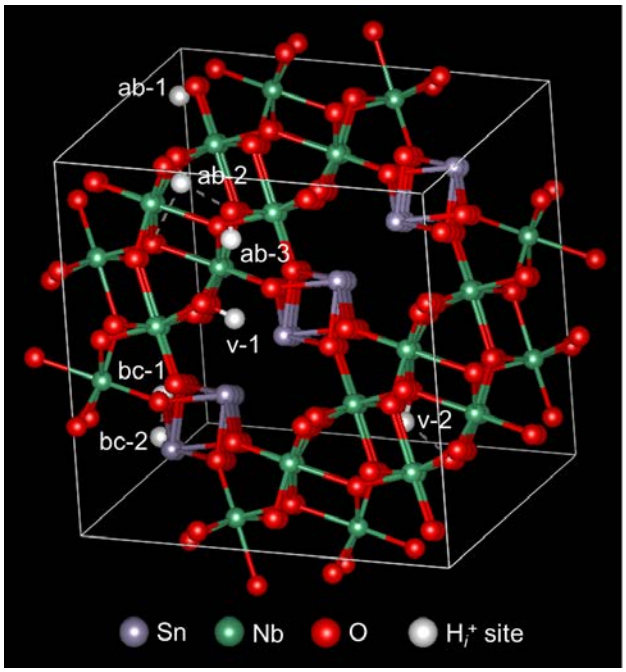

H_i^+ sites	$E - E$(ab-1)
ab-1	-
ab-2	0.27 eV
ab-3	0.13 eV
bc-1	0.01 eV
bc-2	0.14 eV
v-1	0.17 eV
v-2	0. 18 eV

Figure S4. Supercell structure of $SnNb_2O_6$ and the relaxed H_i^+ sites from the considered initial configurations. The labels on H_i^+ sites indicate the types of initial configurations (ab: antibonding sites, bc: bond center sites, v: void sites) The relative energy of each H_i^+ configurations compared to the most stable configuration are shown in the right table.

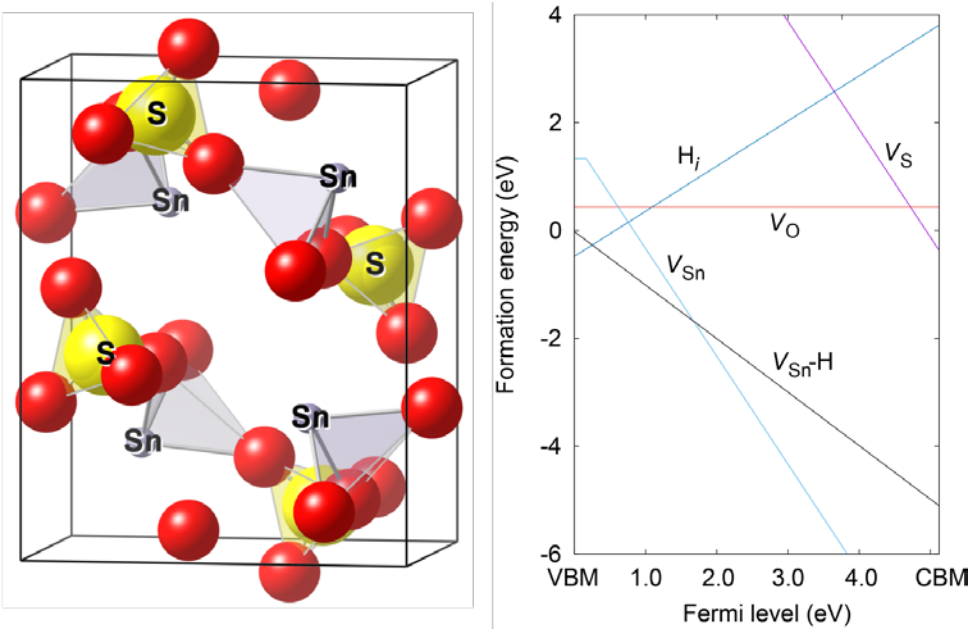

Figure S5. Crystal structure and formation energies of intrinsic and hydrogen-related defects of $SnSO_4$ in the oxygen-rich condition.

Note: The nominal charge of Sn, S, and O in $SnSO_4$ would be +2, +6, and -2, respectively. The high-valence state of S may question the transferability of PAW pseudopotential in which the core shells (1s, 2s, and 2p) are frozen. However, in Ref. S5, Fe(hydro)oxide-H_2O interface with SO_4^{2-} ligand was studied with both VASP and all-electron code (Gaussian) and it was found that the interatomic distances and angles of both calculation agree well with experiments. In another literature, Ref. S6 and Ref. S7 employed the same type of pseudo-potential for materials containing $(SO_4)^{2-}$ and their results showed good agreements with experimental structures and energetics. Therefore, we believe that the VASP PAW potential works well for $SnSO_4$.

Supplementary References

1. Stevanović, V., Lany, S., Ginley, D. S., Tumas, W. & Zunger, A. Assessing capability of semiconductors to split water using ionization potentials and electron affinities only. *Phy. Chem. Chem. Phys.* **16**, 3706–14 (2014).
2. Robertson, J. Band offsets of wide-band-gap oxides and implications for future electronic devices. *J. Vac. Sci. Technol. B* **18**, 1785 (2000).
3. Xiong, K., Robertson, J. & Clark, S. J. Behavior of hydrogen in wide band gap oxides. *J. Appl. Phys.* **102**, 83710 (2007).
4. Pelatt, B. D., Ravichandran, R., Wager, J. F. & Keszler, D. A. Atomic solid state energy scale. *J. Am. Chem. Soc.* **133**, 16852–16860 (2011).
5. Paul, K. W., Kubicki, J. D. & Sparks, D. L. Sulphate adsorption at the Fe (hydr)oxide–H_2O interface: comparison of cluster and periodic slab DFT predictions. *Eur. J. Soil. Sci.* **58**, 978-988 (2017).
6. Derzsi, M., *et al.* Redetermination of crystal structure of $Ag(II)SO_4$ and its high-pressure behavior up to 30 GPa. *Cryst. Eng. Comm.* **15**, 192-198 (2013).
7. Clark, J. M., *et al.* High voltage sulphate cathodes $Li_2M(SO_4)_2$ (M = Fe, Mn, Co): atomic-scale studies of lithium diffusion, surfaces and voltage trends. *J. Mater. Chem. A* **2**, 7446 (2014).